Parity-Time Symmetry in Planar Coupled Magnonic Heterostructures

O.S. Temnaya,[1,*] A.R. Safin,[1,2] D.V. Kalyabin,[1,3] and S.A. Nikitov[1,4,5]

[1] *Kotel'nikov Institute of Radio-Engineering and Electronics of RAS, Moscow 125009, Russia*
[2] *Moscow Power Engineering Institute, Moscow 111250, Russia*
[3] *HSE University, Myasnitskaya Street 20, Moscow, 101000, Russia*
[4] *Moscow Institute of Physics and Technology, Dolgoprudny 141701, Moscow Region, Russia*
[5] *Laboratory "Metamaterials", Saratov State University, Saratov 410012, Russia*

(Received 10 January 2022; revised 16 March 2022; accepted 6 May 2022; published 1 July 2022)

We introduce a theoretical model presenting a *PT*-symmetric system of two planar coupled magnonic ferromagnetic (FM) waveguides covered by thin layers of nonmagnetic metal with a strong spin-orbit interaction [heavy metal (HM)]. The eigenvalues in *PT*-symmetric systems change from real to complex at exceptional points. In magnonics, *PT* symmetry is achieved by a perfect balance of the gain and loss of spin waves. It is possible to control the voltage of exceptional-point appearance in the system by changing the distance between waveguides. The proposed system has a resonance linewidth almost 2 times narrower than that of a single FM-HM heterostructure, thus opening up opportunities for creating highly precise tunable devices, such as detectors and sensors.

DOI: 10.1103/PhysRevApplied.18.014003

I. INTRODUCTION

Recently, several highly informative reviews concerning current research and future directions in magnonics were published [1–4]. In particular, it was stressed that magnonic research is moving toward the advancement of quantum technologies. It is natural for magnonics, since magnons are the quasiparticles associated with collective spin excitations, namely, spin waves [5]. Basic magnonic structures are micro- and nanowaveguides and heterostructures combined with magnetic and nonmagnetic materials. Such structures are extremely important for information processing based on spin waves, as their operating-frequency range lies between units of gigahertz (GHz) and units of terahertz (THz) [6]. This is a unique property, since conventional CMOS technology is restricted by the GHz-frequency range. Spin waves can propagate with little damping in dielectric ferro-, antiferro-, and ferrimagnetic materials over distances with units of microns; moreover, the intrinsic spin-wave damping can be influenced, e.g., by parametric pumping and/or by the spin Hall effect. The energy of spin-wave collective modes can be transferred between coupled magnonic waveguides [7]. Therefore, it is possible to influence this spin-wave transport by changing the intrinsic magnetic damping in waveguides.

A special case, when intrinsic damping in one waveguide is compensated for by antidamping in the other one, which is balanced magnonic loss and gain, constitutes the parity-time (*PT*) symmetric system. The notion of *PT* symmetry came about in 1998 [8]. Originally, it concerned quantum systems with a non-Hermitian Hamiltonian, which, however, could have a real set of eigenstates with real eigenvalues. The *PT*-symmetric Hamiltonian commutes with the parity operator, $\hat{P}$, and the time-reversal operator, $\hat{T}$, i.e., $\hat{P}\hat{T}\hat{H} = \hat{H}\hat{P}\hat{T}$. The action of the parity operator, $\hat{P}$, alters the signs of the coordinate, $\mathbf{r}$, and the momentum, $\mathbf{p}$, thus $\mathbf{r} \to -\mathbf{r}$ and $\mathbf{p} \to -\mathbf{p}$, while the time-reversal operator in change of $\mathbf{p} \to -\mathbf{p}$ and leads to the complex conjugation $i \to -i$. A system described by a Schrödinger-like equation with a complex potential, $U(x)$, is called *PT* symmetric if $U(x)$ has an even real part, $U'(x)$, and an odd imaginary part, $iU''(x)$, i.e., $U'(x) = U'(-x)$ and $U''(x) = -U''(-x)$. The concept of *PT* symmetry attracted strong interest and has been continued by appropriate analogy to various physical systems, such as optics [9,10], electronics [11], acoustics [12], and magnetism [13,14].

A spectrum of a *PT*-symmetric system is generally complex, but it becomes real if the eigenmodes are invariant to the *PT* transformation. The transition point of the system to the *PT*-symmetry-broken phase occurs in the so-called exceptional point (EP), where eigenvalues change from real to complex [15]. When transiting the exceptional point, the eigenmodes and eigenvalues of the system become degenerate. *PT*-symmetric systems constitute, therefore, an exotic class of conservative systems, which simultaneously have properties of dissipative

[*] ostemnaya@gmail.com

systems. Furthermore, the unique nature of the PT-operator spectrum allows us to observe such exciting effects, e.g., single-mode laser generation [16], and steer magnetic permeability at the exceptional points [17].

The transition from a real to a complex spectrum is observed in different systems with equally balanced gain and loss [18,19]. Several PT-symmetric magnonic systems have been demonstrated theoretically [17,20,21] and experimentally [22]. The proposed systems consist of ferromagnetic dielectric films separated by thin layers of metal, which possess a strong spin-orbit interaction (SOI). Balancing of magnonic gain and loss can be achieved in these multilayered structures due to the spin Hall effect (SHE) [23]. The SHE is a phenomenon in which a charge current generates a transverse spin current, so the spin current flows from the metal layer to the ferromagnetic film. Collective spin-wave modes of the magnonic structures can be coupled by exchange and magnetodipolar interactions. In the works mentioned above, an essential contribution to that coupling is provided by Ruderman-Kittel-Kasuya-Yosida (RKKY) interaction between the waveguides, which constitutes the indirect exchange interaction between conduction electrons and nonmagnetic impurities. The main challenge is that it is impossible to create such multilayered structures in which ferromagnetic layers are identical; as previously stated, this is necessary to achieve perfectly balanced magnonic gain and loss.

By contrast, planar PT-symmetric magnonic waveguides have not been explored; they could constitute simpler structures consisting of two (or more) ferromagnetic dielectric films prepared from the same sample (thus, having identical parameters) covered by thin layers of metal with a strong SOI and coupled by a magnetodipolar interaction without indirect exchange. In addition to the requirement imposed on ferromagnetic waveguides, metal layers also have to be identical because an additional metallic layer in a magnetic structure can lead to a shift of the dispersion characteristic. The geometry of planar waveguiding structures is widely used when developing functional electronics elements, such as directional couplers [24,25].

Here, we introduce and investigate planar PT-symmetric heterostructures of "ferromagnetic waveguide-heavy metal" coupled with the magnetodipolar interaction. We first introduce the main concept and the corresponding mathematical model. In Sec. II, we begin with the model in which the equal balance of gain and loss for propagating spin waves is achieved by passing a direct current (dc) through the HM layers. It is possible to control the effective damping of the structure if applying the dc in different directions. We give the principal equations based on the Landau-Lifshitz-Gilbert-Slonczewski (LLGS) model. We consider the case where the external magnetic field, $\mathbf{H}_0$, is perpendicular to the wave vector, $\mathbf{k}$, and lies in the plane of the structure; this corresponds to the surface magnetostatic spin waves (MSSWs). To account for the additional damping associated with the SOI, we add the Slonczewski-Berger term [26] to the LLGS equations, which has a triple vector product of the magnetization vector, $\mathbf{M}$, and the polarization vector of spin current, $\mathbf{p}$, that determines if the effective damping is increased or compensated for. We discuss the obtained mathematical model and expressions in Sec. III. Section IV concludes the paper.

II. PHYSICAL STRUCTURE AND MATHEMATICAL MODEL

The model of the considered system is presented in Fig. 1(a). It consists of two identical ferromagnetic (FM) waveguides covered with thin layers of heavy metal (HM) with a strong SOI. An external magnetic field, $\mathbf{H}_0$, biases both heterostructures. In one waveguide, a microstrip transmission line with frequency ω and power P_{in} excites MSSWs that propagate along the waveguide's central axis. MSSWs can also propagate in the second waveguide due to energy transfer between heterostructures. The energy of the spin waves periodically transfers from one FM waveguide to another, as demonstrated numerically [24] and experimentally [7,25]. Output signals P_{out1} and P_{out2} are detected from both waveguides. When a dc with density J_c flows through a HM layer, a spin current with density J_s directed along the z axis into the FM layer arises due to the SHE. The relationship linking charge and spin-current densities [27] is in the form

$$J_s = \theta_{\text{SH}} J_c = \theta_{\text{SH}} \frac{|V_a|}{\rho L}. \quad (1)$$

Here, θ_{SH} is the spin Hall angle, V_a is the voltage supplied to the HM, ρ is the resistivity of the HM, and L is the distance between the contacts supplied to the HM voltage.

If the polarization vector of the spin current, $\mathbf{p}$, is parallel to the stationary direction of magnetization, $\mathbf{M}_0 = M_s\mathbf{x}$, it is possible to control the spin-wave attenuation at the FM-HM boundary, partially compensating for or amplifying the attenuation by changing the direction and magnitude of J_c [27]. The polarization vector and the direction of stationary magnetization should be parallel to compensate for spin-wave damping and antiparallel to create an additional positive effective damping.

Magnetization dynamics in a FM is described by the Landau-Lifshitz-Gilbert-Slonczewski equation of motion:

$$\frac{d\mathbf{M}}{dt} = -\mu_0|\gamma|[\mathbf{M} \times \mathbf{H}_{\text{eff}}] + \frac{\alpha_G}{M_s}\left[\mathbf{M} \times \frac{d\mathbf{M}}{dt}\right] + \frac{\sigma J_s}{M_s}[\mathbf{M} \times [\mathbf{M} \times \mathbf{p}]], \quad (2)$$

where γ is the gyromagnetic ratio; μ_0 is the vacuum magnetic permeability; $\mathbf{M}$ is the magnetization vector of the

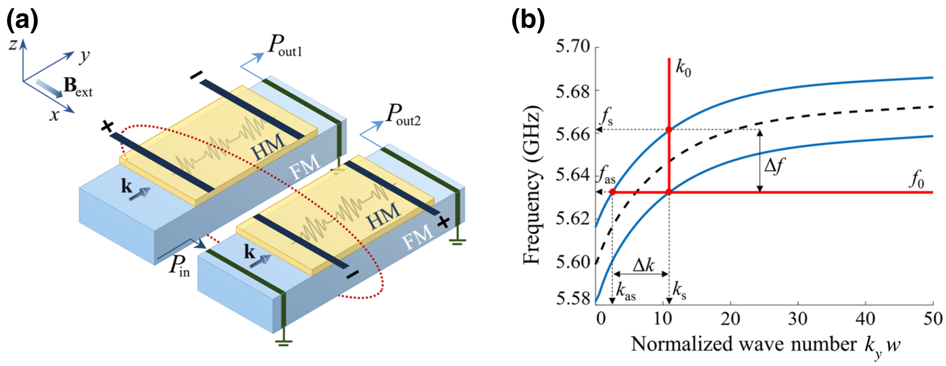

FIG. 1. (a) Coupled FM-HM heterostructures. (b) Dispersion characteristics of isolated and coupled heterostructures. Black dashed line displays the lowest mode of the isolated waveguide; blue solid lines correspond to "symmetric" and "asymmetric" modes of the system of two coupled FM-HM structures.

FM; $\mathbf{H}_{\text{eff}}$ is the effective magnetic field, which includes external, exchange, and demagnetization fields [24]; M_s is the saturation magnetization of the FM, α_G is the Hilbert damping constant, and σ is a phenomenological constant that characterizes the efficiency of spin-transfer torque from the HM to FM. The first term represents the precession of the magnetization vector, $\mathbf{M}$, about the effective magnetic field, $\mathbf{H}_{\text{eff}}$; this is a conservative part of the equation. The second term describes the intrinsic spin-wave damping in FMs (Gilbert damping) related to energy dissipation, and the last term is the Slonczewski-Berger spin-transfer torque from electrons in the HM to magnons in the FM. Effective spin-wave damping can be manipulated by changing the sign of $\mathbf{p}$ in the LLGS equation, which is achieved by variation of the direction of a dc flowing through the HM layer.

Let us consider small oscillations, $\mathbf{m}_\nu(\mathbf{r}, t)$, near the stationary state, $\mathbf{M}_0$, in two coupled FMs, i.e., $\mathbf{m}_\nu = (0, m_{y,\nu}, m_{z,\nu})$. The linearized system of LLGS Eq. (2) can be introduced as follows (in the Fourier representation in terms of k [24]):

$$\frac{d\mathbf{m}_\nu}{dt} = -\boldsymbol{\mu} \times \sum \hat{\Omega}_{\nu\nu'} \cdot \mathbf{m}_{\nu,\nu'} + \alpha_G \left(\boldsymbol{\mu} \times \frac{d\mathbf{m}_\nu}{dt} \right) + \sigma J_s \mathrm{sgn}(-\boldsymbol{\mu} \cdot \mathbf{p}) \mathbf{m}_\nu, \tag{3}$$

where $\boldsymbol{\mu} = \mathbf{x}$, $\omega_H = \gamma \mu_0 H_0$, $\omega_M = \gamma \mu_0 M_s$, $\hat{\boldsymbol{\Omega}}_{\nu\nu'} = (\omega_H + \omega_M \lambda^2 (k_y^2 + \kappa^2)) \delta_{\nu\nu'} \hat{\mathbf{I}} + \omega_M \hat{\mathbf{F}}_{k_y}(d_{\nu\nu'})$, $d_{\nu\nu'}$ is the distance between the waveguides centers, $\kappa = \pi / w_{\text{eff}}$ is the effective wave number, w_{eff} is the effective width of the FM, $\lambda = \sqrt{2A/(\mu_0 M_s^2)}$ is the exchange length, $\delta_{\nu\nu'}$ is Kronecker symbol, and $\hat{\mathbf{I}}$ is the identity matrix. $\hat{\mathbf{F}}_{k_y}(d_{\nu\nu'})$ is the demagnetization coefficient tensor, which consists of the intrinsic demagnetization tensor and the magnetodipolar coupling tensor (here, $\alpha, \beta = x, y$):

$$\hat{\mathbf{F}}_{k_y}(d) = \frac{1}{2\pi} \int \hat{\mathbf{N}}_k e^{ik_x d} dk_x, \tag{4}$$

$$\hat{\mathbf{N}}_{\alpha\beta,k} = \frac{|\sigma_k|^2}{\tilde{w}} \frac{k_{\alpha\beta}}{k^2} f(kt), \ \hat{\mathbf{N}}_{zz,k} = \frac{|\sigma_k|^2}{\tilde{w}} (1 - f(kt)). \tag{5}$$

Here, $f(kt) = 1 - (1 - \exp(-kt))/kt$, t is the waveguide thickness, $\sigma_k = \int_{-w/2}^{w/2} m(x) \exp(-ik_x x) dx$ is the spin-wave profile across the waveguide thickness in the Fourier representation, $\tilde{w} = \int_{-w/2}^{w/2} m(x)^2 dx$ is the normalized constant of the mode profile $m(x)$. The magnetodipolar self-interaction of each waveguide can be calculated by assuming that $\hat{\mathbf{F}}_{k_y}(0)$, and the magnetodipolar interaction between waveguides corresponds to $\hat{\mathbf{F}}_{k_y}(d)$, where $d = w + \delta$, w is the width of the waveguide, and δ is the gap between waveguides. Diagonal coefficients of the tensor $\hat{\boldsymbol{\Omega}}_{\nu\nu'}$ therefore describe the self-interaction of each waveguide, and the coefficients of magnetodipolar coupling between waveguides are $\tilde{\Omega}_{xx} = \omega_M \hat{\mathbf{F}}_{k_y}^{xx}(d)$ and $\tilde{\Omega}_{zz} = \omega_M \hat{\mathbf{F}}_{k_y}^{zz}(d)$.

The dispersion characteristic of an isolated FM waveguide with damping related to the spin-transfer torque, $\Gamma_{\text{I}} = \sigma J_s \mathrm{sgn}(-\boldsymbol{\mu} \cdot \mathbf{p})$, is described by the expression $\omega_0(k_y) = \omega' + i\omega''$, where $\omega' = \sqrt{\Omega_{xx}\Omega_{zz}}$, $\omega'' = \sqrt{0.5\alpha_G(\Omega_{xx} + \Omega_{zz}) - \Gamma_I}$. If one introduces the effective spin-wave damping in FMs in the form $\Delta\Gamma_1 = \alpha_G \Omega_{xx} + \Gamma_I$, $\Delta\Gamma_2 = \alpha_G \Omega_{zz} - \Gamma_I$ acting on m_y and m_z components, respectively, the system of linearized LLGS equations can be written as follows:

$$\begin{cases} \dot{m}_{y,\nu\nu'} = \Omega_{zz} m_{z,\nu\nu'} + \Delta\Gamma_{\nu,\nu'} m_{y,\nu\nu'} + \tilde{\Omega}_{zz} m_{z,\nu'\nu}, \\ \dot{m}_{z,\nu\nu'} = -\Omega_{xx} m_{y,\nu\nu'} + \Delta\Gamma_{\nu,\nu'} m_{z,\nu\nu'} - \tilde{\Omega}_{xx} m_{y,\nu'\nu}. \end{cases} \tag{6}$$

To solve the system in Eq. (6), let us introduce complex amplitudes, $\dot{c} = am_y + ibm_z$, $m_y = (c + c^*)/2a$, $m_z = (c - c^*)/2ib$. Here, we choose constants $a =$

$\sqrt{\Omega_{xx}/\Omega}$ and $b = \sqrt{\Omega_{zz}/\Omega}$ to diagonalize the system in Eq. (6), so that the linearized equations for the magnetization dynamics in each waveguide, without taking into account damping, take the form $\dot{c}_v = -i\Omega c_v$. After transformations, the system in Eq. (6) can be written as

$$\dot{c}_v = -i\Omega c_v - \Gamma_v c_v - i\Omega_c c_{v'}, \tag{7}$$

where $\Gamma_{1,2}$ are the damping coefficients for both waveguides:

$$\Gamma_{1,2} = \alpha_G \frac{\Omega_{xx} + \Omega_{zz}}{2} \pm \Gamma_{\mathrm{I}}, \tag{8}$$

and the coupling constant is

$$\Omega_c = \tilde{\Omega}_{zz}\sqrt{\frac{\Omega_{xx}}{\Omega_{zz}}} + \tilde{\Omega}_{xx}\sqrt{\frac{\Omega_{zz}}{\Omega_{xx}}}. \tag{9}$$

Diagonalizing Eq. (7), we obtain expressions for eigenvalues in the form

$$\lambda_{1,2} = \omega_0 - i\Gamma_0 \pm \sqrt{\Omega_c^2 - \Gamma_{\mathrm{I}}^2}. \tag{10}$$

As one can see from Eq. (10), two eigenvalues, $\lambda_{1,2}$, coalesce to $\lambda_0 = \omega_0 - i\Gamma_0$ when

$$\Gamma_I|_{\mathrm{EP}} = \Omega_c. \tag{11}$$

The considered expression for Eq. (11) is the condition for the existence of an EP in which eigenmodes and eigenvalues are degenerate. The effective antidamping, Γ_I, should change in both waveguides to the value Ω_c. The real part of the eigenvalues, $Re\lambda_{1,2} = \omega_0$, does not change when increasing $\Delta\Gamma$, and the imaginary part splits into two nondegenerate values: $\mathrm{Im}\lambda_{1,2} = -\Gamma_0 \pm \sqrt{\Gamma_{\mathrm{I}}^2 - \Omega_c^2}$.

III. RESULTS AND DISCUSSION

Let us consider processes occurring in coupled FM waveguides without taking into account the spin current. Dispersion characteristics of isolated waveguides split into symmetric and asymmetric branches due to magnetodipolar interactions, as shown in Fig. 1(b). These branches are located symmetrically near the corresponding eigenmodes, i.e., modes of isolated waveguides. The magnetodipolar interaction between waveguides weakens with increasing wave number and the exchange interaction becomes prevalent, with normal modes striving towards eigenmodes. Splitting of the spectrum into two normal modes is observed experimentally in micro- and nanowaveguides [25,28].

When the spin current arises in the HM layers due to the SHE, the spin-wave amplitudes can increase in gain or be attenuated, depending on the mutual polarization of vectors $\boldsymbol{\mu}$ and $\mathbf{p}$. As mentioned before, the dispersion characteristics of magnonic systems, in which intrinsic spin-wave damping is equally compensated for by antidamping, can have exceptional points where the eigenmodes and eigenvalues coalesce. To observe the effect of exceptional-point position on the dispersion characteristics, one should increase effective damping in one FM waveguide and equally decrease it in another waveguide by applying a voltage to the HM layers in a particular way [see Fig. 1(a)]. The condition for exceptional-point appearance can be found from Eq. (1); the equation for complex amplitudes, $c_{1,2}$, Eq. (7); and characteristic Eq. (10). The expression for a critical voltage, V_{EP}, at which the exceptional point occurs can be obtained from Eqs. (1) and (11) in the form

$$V_{\mathrm{EP}}(d) = \Omega_c(d)\rho L/\sigma\theta_{\mathrm{SH}}. \tag{12}$$

Here, $\Omega_c(d)$ is the distance-dependent effective coupling parameter, which is determined from Eq. (9). We use the following physical parameters for calculations: width of waveguides, $w = 20$ μm; distance between contacts, $L = 3.5$ μm; the gap between waveguides lies in the range of $\delta = 5 - 30$ μm; saturation magnetization, $M_s =$ 140 kA/m; $\mu_0 = 1.25 \times 10^{-6}$ H/m; $\gamma = 2\pi \times 28$ GHz/T; $\omega_H = \omega_M$; Gilbert damping, $\alpha_G = 2 \times 10^{-4}$; spin Hall angle, $\theta_{\mathrm{SH}} = 0.076$; resistivity of the HM, $\rho = 371$ nΩ; and $\sigma = 1.03 \times 10^{-2}$ m^2 Hz/A. Figure 2(a) shows the dependence of the critical voltage, V_{EP}, on the distance between heterostructures. As the distance between heterostructures increases, the critical voltage decreases; this is associated with attenuation of the magnetodipolar coupling between the structures. The inset in Fig. 2(a) shows the dependence of the real and imaginary parts of the frequency on the voltage applied to the metal. The dependencies of V_{EP} on the normalized wave number and the distance between waveguides are shown in Fig. 2(b). The critical voltage increases with decreasing distances, and the eigenmode range is reduced. The exchange interaction becomes prevalent over the magnetodipolar interaction upon reducing the wave number, so observation of the exceptional point is no longer possible. When the distance between waveguides is fixed, V_{EP} has a maximum value that corresponds to the normalized wave number, as shown in Fig. 2(b).

An essential characteristic of the exceptional points is that not only the eigenvalues but also the corresponding eigenvectors are degenerate [8]. In Hermitian systems, the eigenvalue spaces have a double-cone topology with degeneracy points on the cone vertexes. By contrast, in non-Hermitian systems, the eigenvalue space represents the Riemann sheets centered near the exceptional points [15]. This unique characteristic allows the creation of hypersensitive sensors based on PT-symmetric physical

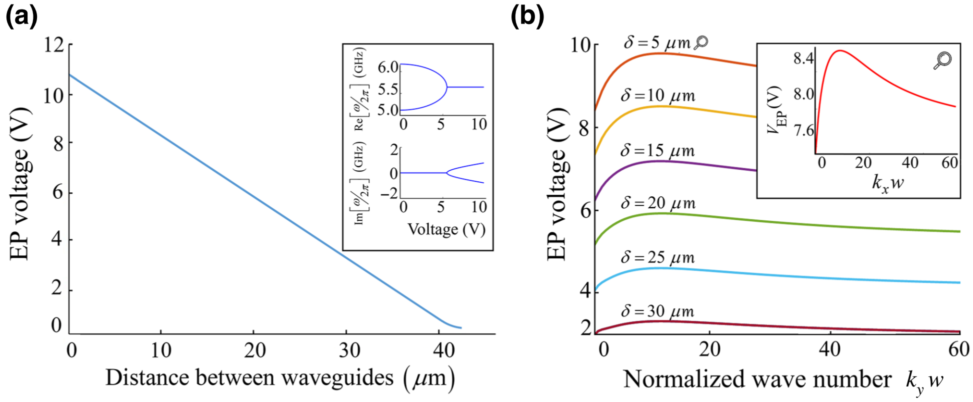

FIG. 2. Dependence of the exceptional-point voltage as a function of (a) the distance between waveguides and (b) the normalized wave number, $k_y w$, for different gaps between waveguides, δ. Inset in (a) shows the dependence of normal modes on the voltage supplied to the HM. Inset in (b) shows the scaled dependence of the exceptional-point voltage on normalized wave number for the case when $\delta = 5\ \mu$m.

structures [29]. These structures, indeed, have a strikingly narrow resonance curve. To demonstrate this, let us solve the system of spin-wave amplitudes, Eq. (7), with an external influence in the form of $e^{-i\omega t}$. Seeking the solution of the system in the form $c_v = A_v e^{-i\omega t}$ and using the separation of variables method, one can obtain expressions for amplitudes normalized to the exceptional point. They are $(1 + (2D/\Gamma_0)^2)^{-0.5}$ and $(1 + (D/\Gamma_0)^2)^{-1}$ on the left- and right-hand sides of the exceptional point in parametric space, respectively, and $D = \sqrt{\Omega_c^2 - \Gamma_I^2}$. According to Eq. (1), the spin-current density that corresponds to $V_{\rm EP}$ is $J_s = 3.2 \times 10^7$ A/cm^2. The resonance-amplitude dependence as a function of voltage and frequency is shown in Fig. 3(a). The nonsymmetric character of the dependency at the left and the right sides is related to the eigenmode degeneracy. The highest-voltage value corresponds to the $V_{\rm EP}$ voltage. The resonance linewidth of the PT-symmetric system is $\Delta\omega = 2\Gamma_0\sqrt{\sqrt{2}-1} \approx 0.6\Delta\omega_0$, where $\Delta\omega_0 = 2\Gamma_0$ is the spin-wave resonance linewidth of a single FM-HM heterostructure. Thus, the resonance linewidth of the system *at the exceptional point* is almost half of the spin-wave-resonance linewidth of one FM-HM heterostructure [see Fig. 1(b)].

IV. CONCLUSION

In this work, we describe planar PT-symmetric magnonic FM-HM heterostructures with balanced gain and loss. We use the method of controlling efficient damping in waveguides based on the SHE; to reach it, we vary the value of the dc applied to the HM, which is the way to change the exceptional-point position. In the system composed of two coupled FM-HM heterostructures, in one of them, effective damping is compensated for by carrying the spin-transfer torque from the HM to the FM. In another structure, effective damping is increased by reversing the direction of the dc applied to the HM. We demonstrate that increasing the distance between waveguides decreases the voltage of exceptional-point appearance and the coupling strength also decreases. We show that the studied

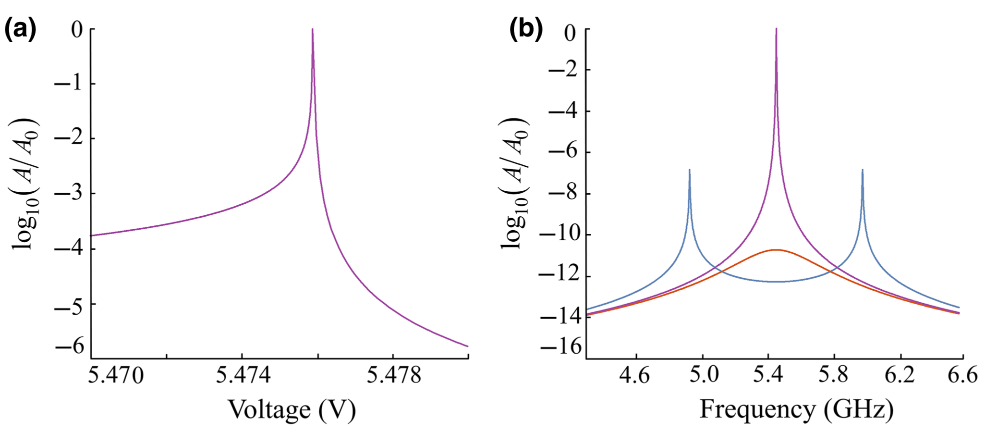

FIG. 3. Resonance-amplitude dependency on (a) input voltage and (b) normal-mode frequencies. Maximum voltage value corresponds to $V_{\rm EP}$; blue peaks on the right correspond to voltages on the left of the exceptional point; red line is the partial frequency on the right of the exceptional point.

system has a very narrow resonant-amplitude dependence on voltage, which shows the specific nature of the exceptional point. The resonance linewidth of the studied system is almost half of the spin-wave resonance linewidth of a partial HM-FM heterostructure. The magnetic oscillation amplitude grows significantly near the exceptional point; therefore, nonlinear effects may play an essential role in the system (see the Appendix). This goes beyond the scope of our work and must be the subject of a separate study. Results of this work can be used to create coupled planar magnonic waveguides with local control of effective damping achieved in various ways. It would be possible to create high-precision devices, such as sensors and detectors, using the proposed system.

ACKNOWLEDGMENTS

We would like to acknowledge support from the Government of the Russian Federation for state support of scientific research conducted under the guidance of leading scientists in Russian higher education institutions, research institutions, and state research centers of the Russian Federation (Project No. 075-15-2019-1874). A.R. acknowledges support from the Russian Science Foundation (Grant No. 21-79-10396). D.V. acknowledges support from a Grant of the President of the Russian Federation for the young scientist (Grant No. MK-61.2021.1.2).

APPENDIX: ESTIMATION OF NONLINEAR EFFECTS

Let us estimate the influence of nonlinear effects on the growth of the amplitude at the exceptional point. Indeed, as shown earlier, the amplitudes of magnetic oscillations in magnonic waveguides sharply increase at the EP. We consider the effect of nonlinearity by adding appropriate coefficients to the system of Eq. (7). These reflect the limitations of longitudinal components of magnetization vectors at sufficiently large values of external-signal amplitudes. We take into account the nonlinear terms that appear in the equations for complex amplitudes, Eq. (7), by adding them to the last expression in the following form [30]:

$$\dot{c}_1 + i\Omega c_1 + \Gamma_0(1 + Q|c_1|^2)c_1 - \Gamma_\mathrm{I} c_1 = i\Omega_c c_2 + \Lambda_0 e^{-i\omega t},$$
$$\dot{c}_2 + i\Omega c_2 + \Gamma_0(1 + Q|c_2|^2)c_2 + \Gamma_\mathrm{I} c_2 = i\Omega_c c_1, \qquad \text{(A1)}$$

where Q is a dimensionless parameter describing nonlinear relaxation, most often found phenomenologically from experimental data [30,31]; Γ_0 is a linear relaxation rate of the uniform magnetization precession; and Λ_0 is the amplitude of the external signal. Notably, the system in Eq. (A1) does not include the nonlinear coefficient reflecting the ferromagnetic-resonance-frequency shift, which characterizes the effect of nonisochronism—the dependence of the oscillation frequency on the amplitude. It can be neglected

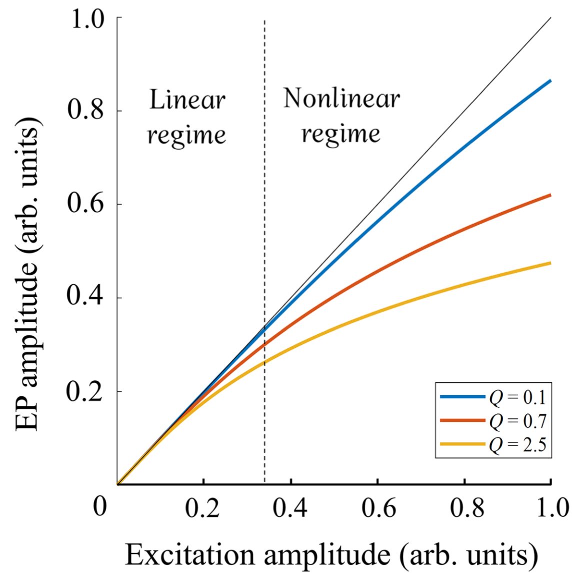

FIG. 4. Dependence of EP amplitude on excitation amplitude.

by selecting an appropriate magnetic field magnitude and its direction.

Here, we consider the influence of the introduced coefficient Q on the change in the amplitudes of the oscillations at the EP when varying this coefficient. The corresponding dependence is shown in Fig. 4. With an increase in the amplitude of the external signal, the oscillation amplitude is limited, and it decreases with an increase of the nonlinearity parameter. Therefore, the increase in the oscillation amplitude at the EP is limited by the system's nonlinearity. Notably, all the dependencies obtained in this work are plotted with a linear model.

[1] A. Barman, G. Gubbiotti, S. Ladak, A. O. Adeyeye, M. Krawczyk, J. Gräfe, C. Adelmann, S. Cotofana, A. Naeemi, V. I. Vasyuchka, *et al.*, The 2021 magnonics roadmap, J. Phys.: Condens. Matter **33**, 413001 (2021).

[2] A. V. Chumak, P. Kabos, M. Wu, C. Abert, C. Adelmann, A. Adeyeye, J. Åkerman, F. G. Aliev, A. Anane, A. Awad, *et al.*, Roadmap on spin-wave computing, arXiv:2111.00365v1 (2021).

[3] D. D. Awschalom, C. R. Du, R. He, F. J. Heremansi, A. Hoffmann, J. Hou, H. Kurebayashi, Y. Li, L. Liu, V. Novosad, *et al.*, Quantum engineering with hybrid magnonic systems and materials, IEEE Trans. Quantum. Eng. **2**, 5500836 (2021).

[4] Y.-P. Wanga and C.-M. Hu, Dissipative couplings in cavity magnonics, J. Appl. Phys. **127**, 130901 (2020).

[5] S. A. Nikitov, D. V. Kalyabin, I. V. Lisenkov, A. N. Slavin, Yu. N. Barabanenkov, S. A. Osokin, A. V. Sadovnikov, E. N. Beginin, M. A. Morozova, Yu. P. Sharaevsky, *et al.*,

Magnonics: A new research area in spintronics and spin wave electronics, Phys.-Usp. **58**, 1002 (2015).

[6] S. A. Nikitov, A. R. Safin, D. V. Kalyabin, A. V. Sadovnikov, E. N. Beginin, M. V. Logunov, M. A. Morozova, S. A. Odintsov, S. A. Osokin, A. Yu. Sharaevskaya, *et al.*, Dielectric magnonics: From gigahertz to terahertz, Phys.-Usp. **63**, 945 (2020).

[7] A. V. Sadovnikov, S. A. Odintsov, E. N. Beginin, A. A. Grachev, V. A. Gubanov, S. E. Sheshukova, Yu. P. Sharaevskii, and S. A. Nikitov, Nonlinear spin wave effects in the system of lateral magnonic structures, JETP Lett. **107**, 1 (2018).

[8] C. M. Bender and S. Boettcher, Real Spectra in Non-Hermitian Hamiltonians Having *PT*-Symmetry, Phys. Rev. Lett. **80**, 5243 (1998).

[9] R. El-Ganainy, K. G. Makris, D. N. Christodoulides, and Ziad H. Musslimani, Theory of coupled optical *PT*-symmetric structures, Opt. Lett. **32**, 17 (2007).

[10] A. A. Zyablovsky, A. P. Vinogradov, A. A. Pukhov, A. V. Dorofeenko, and A. A. Lisyansky, *PT*-symmetry in optics, Phys.-Usp. **57**, 11 (2014).

[11] J. Schindler, Z. Lin, J. M. Lee, H. Ramezani, F. M. Ellis, and T. Kottos, *PT*-symmetric electronics, J. Phys. A: Math. Theor. **45**, 444029 (2012).

[12] P. Deymier, *Acoustic Metamaterials and Phononic Crystals* (Springer, Berlin, 2013).

[13] A. Galda and V. M. Vinokur, Parity-time symmetry breaking in magnetic systems, Phys. Rev. B **94**, 020408 (2016).

[14] H. Liu, D. Sun, C. Zhang, M. Groesbeck, R. McLaughlin, and Z. V. Vardeny, Observation of exceptional points in magnonic parity-time symmetry devices, Sci. Adv. **5**, 11 (2019).

[15] M.-A. Miri and A. Alù, Exceptional points in optics and photonics, Science **363**, 6422 (2019).

[16] I. V. Doronin, A. A. Zyablovsky, E. S. Andrianov, A. A. Pukhov, and A. P. Vinogradov, Lasing without inversion due to parametric instability of the laser near the exceptional point, Phys. Rev. A **100**, 021801(R) (2019).

[17] X.-G. Wang, G.-H. Guo, and L. Berakdar, Steering magnonic dynamics and permeability at exceptional points in a parity–time symmetric waveguide, Nat. Comm. **11**, 5663 (2020).

[18] A. Guo, G. J. Salamo, D. Duchesne, R. Morandotti, M. Volatier-Ravat, V. Aimez, G. A. Siviloglou, and D. N. Christodoulides, Observation of *PT*-Symmetry Breaking in Complex Optical Potentials, Phys. Rev. Lett. **103**, 093902 (2009).

[19] Y. Yang, H. Jia, Y. Bi, H. Zhao, and J. Yang, Experimental Demonstration of an Acoustic Asymmetric Diffraction Grating Based on Passive Parity-Time-Symmetric Medium, Phys. Rev. Appl. **12**, 034040 (2019).

[20] J. M. Lee and T. Kottos, Macroscopic magnetic structures with balanced gain and loss, Phys. Rev. B **91**, 094416 (2016).

[21] X.-G. Wang, G.-H. Guo, and L. Berakdar, Enhanced Sensitivity at Magnetic High-Order Exceptional Points and Topological Energy Transfer in Magnonic Planar Waveguides, Phys. Rev. Appl. **15**, 034050 (2021).

[22] S. Wittrock, S. Perna, R. Lebrun, R. Dutra, R. Ferreira, P. Bortolotti, C. Serpico, and V. Cros, Exceptional points controlling oscillation death in coupled spintronic nano-oscillators, arXiv:2108.04804 (2021).

[23] M. I. Dyakonov and A. V. Khaetskii, *Spin Hall Effect* (Springer-Verlag, Berlin, Heidelberg, 2008).

[24] Q. Wang, P. Pirro, R. Verba, A. Slavin, B. Hillebrands, and A. Chumak, Reconfigurable nanoscale spin-wave directional coupler, Sci. Adv. **4**, 1 (2018).

[25] Q. Wang, M. Kewenig, M. Schneider, R. Verba, F. Kohl, B. Heins, M. Geilen, M. Mohseni, *et al.*, A magnonic directional coupler for integrated magnonic half-adders, Nat. Electron. **3**, 765 (2020).

[26] J. C. Slonczewski, Current-driven excitation of magnetic multilayers, J. Magn. Magn. Mater. **159**, 1 (1996).

[27] Z. Wang, Y. Sun, M. Wu, V. Tiberkevich, and A. Slavin, Control of Spin Waves in a Thin Film Ferromagnetic Insulator through Interfacial Spin Scattering, Phys. Rev. Lett. **107**, 146602 (2011).

[28] A. V. Sadovnikov, E. N. Beginin, S. E. Sheshukova, D. V. Romanenko, Yu. P. Sharaevskii, and S. A. Nikitov, Directional multimode coupler for planar magnonics: Side-coupled magnetic stripes, Appl. Phys. Lett. **107**, 202405 (2015).

[29] J. Wiersig, Review of exceptional point-based sensors, Photonics Res. **8**, 9 (2020).

[30] A. Slavin and V. Tiberkevich, Excitation of spin waves by spin-polarized current in magnetic nano-structures, IEEE Trans. Magn. **44**, 7 (2008).

[31] S. R. Lake, B. Divinskiy, G. Schmidt, S. O. Demokritov, and V. E. Demidov, Interplay between Nonlinear Spectral Shift and Nonlinear Damping of Spin Waves in Ultrathin Yttrium Iron Garnet Waveguides, Phys. Rev. Appl. **17**, 034010 (2022).